Extended Abstracts of the 1994 International Conference on Solid State Devices and Materials, Yokohama, 1994, pp. 811-813

PC-2-1

Hydrogenation Effects in $Hg_{1-x}Cd_xTe$ Layers Grown on p-CdTe(211)B Substrates by Molecular Beam Epitaxy

M. D. Kim, M. S. Han, and T. W. Kang[a)]
Department of Physics, Dongguk University, Seoul 100-715, Korea
J. M. Kim, H. K. Kim, Y. T. Jeoung
Agency for Defence Development, Daejon 300-600, Korea
T. W. Kim
Department of Physics, Kwangwoon University, Seoul 139-701, Korea
J. B. Choi
Department of Physics, Chungbuk National University, Cheongju, 360-763, Korea

Abstract

Fourier transform infrared (FTIR) and Hall effect measurements have been carried out to investigate the hydrogen effects on the defects existing in nominally undoped $Hg_xCd_{1-x}Te$ grown by molecular beam epitaxy on undoped p-CdTe (211) B-orientation substrates. After hydrogenation, the results of the FTIR spectra showed that the transmittance intensity was rasied by as much as about 5 times in comparison to the as-grown $p-Hg_{1-x}Cd_xTe$, and that the absorption edge shifted to the short wavelength range. Hall effect measurements showed that the resistivity and mobility of the $n-Hg_{1-x}Cd_xTe$ after hydrogenation were raised in comparison to the as-grown $n-Hg_{1-x}Cd_xTe$. P-type $Hg_{1-x}Cd_xTe$ was converted to n-type $Hg_{1-x}Cd_xTe$ by hydrogenation. The increase of the transmittance intensity after hydrogenation is considered to be due to impurities or defects being passivated by hydrogen atoms.

I. Introduction

The role of the hydrogen atom is attractive because of the significant improvement in the electrical and optical properties of semiconductors caused by its injection into those materials. Since the hydrogen atoms can passivate the electrical behavior of dangling or defective bonds, the existence of these bonds in single-crystal and polycrystalline semiconductors is very interesting [1]. The improvement of the electrical and optical properties of these materials has been observed from the enhancement of the photoluminescence intensity [2, 3] and the elecron mobility [4, 5]. However, most hydrogenation studies of semiconductors were performed on GaAs and Si [6, 7]; and even though Chen et al. [8] reported hydrogen passivation on $Hg_{1-x}Cd_xTe$, very little work has been performed on $Hg_{1-x}Cd_xTe$ semiconductors. The detailed mechanism of the improvement in the crystallinity of the $Hg_{1-x}Cd_xTe$ semiconductors by hydrogenation has still to be investigated.

This paper reports reflection high-energy electron diffraction (RHEED) measurements which were performed to investigate the interface atomic structure and Fourier transform infrared (FTIR) and Hall effect measurements which were performed in order to investigate the effect of hydrogenation for nominally undoped $Hg_{1-x}Cd_xTe$ grown on nominally undoped p-CdTe (211) B-orientation substrates by molecular beam epitaxy (MBE). The results of these measurements show that hydrogen passivation not only improves the quailty of the materials but also clarifies the physical origin of those materials.

II. Experimental Details

The carrier concentration of the nominally undoped p-CdTe (211) B-orientation substrates used in this experiment was $0.5 - 2 \times 10^{15}$ cm^{-3}. The samples were degreased successively in trichlorethylene, acetone, and methanol at 60℃ for 15 min, and etched with a mixture of methanol and bromine with a bromine concentration of 1 % for 60 sec. After the wafers were cleaned chemically, they were mounted onto a molybdenum susceptor by soldering using indium. Before $Hg_xCd_{1-x}Te$ growth, the CdTe substrates were thermally cleaned at 310℃ in a Te_2 atmosphere. The deposition was done in the substrate termperature range from 185 to 190℃, and the typical growth rate was approximately 3 Å/sec. Using a capacitively coupled rf (13.56 MHz) enhanced chemical vapor deposition, the $Hg_xCd_{1-x}Te$ (x = 0.2 and 0.3) layers were exposed to a hydrogen plasma with power densities of 0.1, 0.15, and 0.3 W/cm^2 at a pressure of 0.9 Torr for 60 min at 50℃. The carrier concentration and mobility of the $n-Hg_{0.8}Cd_{0.2}Te$ layer at 77 K were 3.3×10^{15} cm^{-3} and 1.2×10^5 cm^2/V-s, respectively, and those of the $p-Hg_{0.7}Cd_{0.3}Te$ layer at 77 K were 9×10^{15} cm^{-3} and 286 cm^2/V-s, respectively. The thicknesses of the $n-Hg_{0.8}Cd_{0.2}Te$ and $p-Hg_{0.7}Cd_{0.3}Te$ layers were 6 and 20 μm, respectively.

III. Results and Discussion

The results of the 35-keV RHEED patterns observed in the [110] GaAs azimuth are shown in Figs. 1-(a) and 1-(b). Figure 1-(a) shows a milky streaky pattern for the CdTe (211) B deoxidized; this behavior indicates that the surface defects at the CdTe (211) B surface are created due to the Te outgassing from the CdTe (211) B surface. The RHEED pattern for a 6-μm Hg$_{0.8}$Cd$_{0.2}$Te layer on a CdTe (211) B substrtate is shown in Fig. 1-(b). The structure of the RHEED pattern is streaky, and this implies that a clear two-dimensional growth has reconstructed on CdTe (211) B. A surface morphology of a 6-μm Hg$_{0.8}$Cd$_{0.2}$Te layer grown on CdTe (211) B is shown in Fig. 1-(c), and the as-grown Hg$_{0.8}$Cd$_{0.2}$Te film has a mirror-like surface.

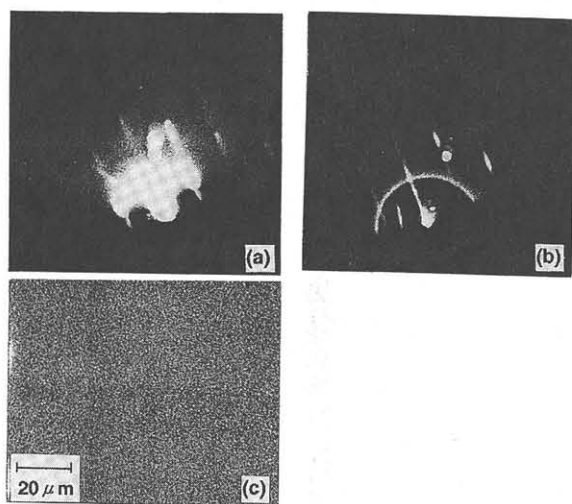Fig. 1. Reflection high-energy electron diffraction patterns for the (211) plane along [0$\bar{1}$1] axis: (a) CdTE (211) B deoxidized, (b) a 6-μm Hg$_{0.8}$Cd$_{0.2}$Te layer grown on CdTe (211) B, and (c) a surface morphology of a 6-μm Hg$_{0.8}$Cd$_{0.2}$Te layer grown on CdTe (211) B.

Figures 2-(a) and 2-(b) show the optical micrographs for the as-grown and the hydrogenated n-Hg$_{0.8}$Cd$_{0.2}$Te layers on CdTe (211) B, respectively. The V-type defects appear as micropairs with two defect planes, and they exist in a (111) plane. The formation of these defects originates from the created Te layer at initial stages of the Hg$_{1-x}$Cd$_x$Te layer growth, and a columnar polycrystalline Hg$_{1-x}$Cd$_x$Te layers might be formed at the inner side of these defects [9]. When Hg compounds do not adsorbed on a microtwin plane, Te layers are formed on that side. The Te clusters creat the microtwins according to the (111) plane, and form new type of the clusters. The formation of the new clusters produces the V-type defects with the polycrystalline at the inner side. When the density and thickness of the Te layer are sufficiently large, the Hg$_{1-x}$Cd$_x$Te layer becomes a polycrystalline resulting from the overlapping of the V-type defects [9]. After hydrogenation, the dark spots appeared resulting from the Hg outgassing at the edges of the V-type defects, and the appearance of the spots was caused by the Te precipitates.
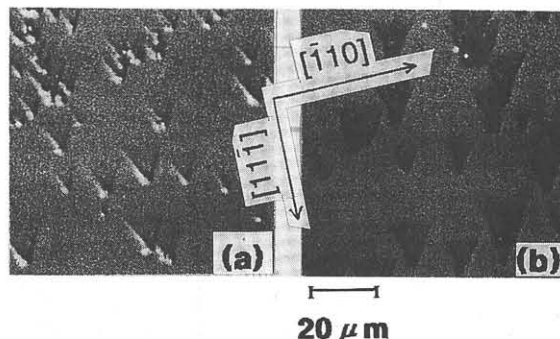

Fig. 2. Optical micrographs for (a) as-grown (b) hydrogenated n-Hg$_{0.8}$Cd$_{0.2}$Te layers grown on CdTe (211) B.

Figure 3 shows the transmittance spectra for the as-grown and n-Hg$_{0.8}$Cd$_{0.2}$Te layers hydrogenated with power densities of 0.1 and 0.15 W/cm^2 at 50 ℃. The relationship between the absorption coefficient (α) and the transmittance (T) obeys the following equation :

$$T = \frac{(1-R)^2 e^{-\alpha d}}{1-R^2 e^{-2\alpha d}} \qquad (1)$$

where d is the thickness of the sample, and R is the reflectance. As the power density of the hydrogenation becomes larger, the absorption edges shift to the short wavelength, and the intensity of the transmittance for the photon energy in a energy gap increases.

Figure 4 shows the transmittance spectra for the as-grown and a n-Hg$_{0.8}$Cd$_{0.2}$Te layer hydrogenated with a power density of 0.3 W/cm^2 at 50 ℃. After hydrogenation, the absorption edges shift to the short wavelength, and the intensity of the transmittance spectrum increases.

Figure 5 shows the transmittance spectra for the as-grown and a p-Hg$_{0.7}$Cd$_{0.3}$Te layer hydrogenated with a power density of 0.3 W/cm^3 at 50 ℃. After the p-Hg$_{0.7}$Cd$_{0.3}$Te was hydrogenated, the transmittance increases, and the absorption edge shifts to the short wavelength range.

In addition to FTIR measurements, Hall effect measurements were carried out to determine the carrier concentration, the mobility, and the resistivity in the hydrogenated samples. Figure 6 shows the carrier concentration and mobility in as-grown and hydrogenated n-Hg$_{0.8}$Cd$_{0.2}$Te as a function of temperature. While the carrier concentration of the hydrogenated n-Hg$_{0.8}$Cd$_{0.2}$Te was lowered
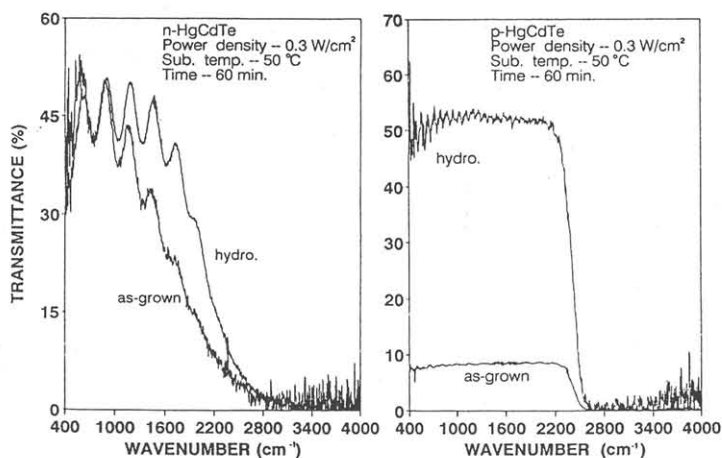
Fig. 4. Fourier transform infrared spectra for as-grown and n-Hg₀.₈Cd₀.₂Te layers hydrogenated with power densities of 0.3 at 50℃.

Fig. 5. Fourier transform infrared spectra for as-grown and p-Hg₀.₇Cd₀.₃Te layers hydrogenated with power densities of 0.1 and 0.15 W/cm² at 50℃.
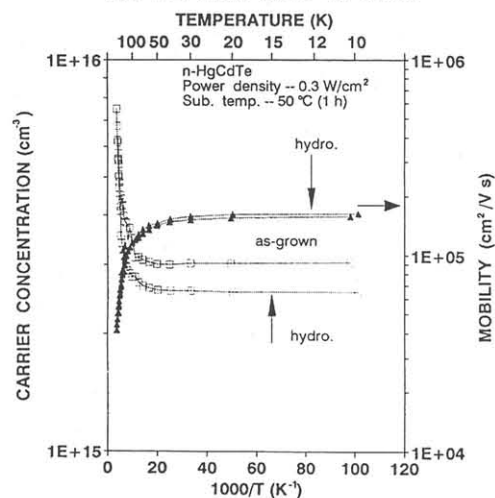

Fig. 6. Carrier concentrations and mobilities in as-grown and n-Hg₀.₈Cd₀.₂Te hydrogenated with a power density of 0.3 W/cm² at 50℃ as a function of the temperature.

by 2.7×10^{15} cm^{-3}, the mobility increased slightly. The resistivities of the samples as a function of the temperature measured by Hall effect measurements are shown in Fig. 7. The resistivity in hydrogenated n-Hg₀.₈Cd₀.₂Te increases in comparison with the as-grown one. The variation of the carrier concentration, the mobility, and the resistivity are caused by the decrease of the Hg vacancy defects resulting from the occupation of the Hg vacancies by hydrogen atoms.

The electrical and optical properties of the Hg₁₋ₓCdₓTe alloy are affected by the spot defects, the extended defects, and the residual impurities. Since the Hg₁₋ₓCdₓTe has small energy gap and small effective mass, the impurity bands or defect bands created by a small amount of the impurities or defects

contributes the state tail density. The impurity concentration can be explained using a hydrogenic model, and the effective Bohr radius of the electron bound in the impurity atom is given by

$$a = 5.29 \times 10^{-9} \varepsilon_0 m/m^* \quad (cm) \qquad (2)$$

where m is the free electron mass, m* is the electron effective mass, and the ε_0 is the dielctric constant. When electron wavefunctions were confined by the superposition of two neighbor impurities, impurity bands were created. When the impurity concentration is above $3 \pi a^3/4$ ($\simeq 10^{14}$ cm^{-3}), the impurity bands were created. The exponential absorption tails induced by the defects and impurities were observed in the HgₓCd₁₋ₓTe alloy [10, 11]. If the behavior of the absorption edge varies the existence of the defects in the materials, the absorption edge is dependent on the carrier concentration of the defect [10]. Thus, the increase of the transmittance after hydrogenation is considered to be due to the Hg vacancies being passivated by a hydrogen atom, and the shift of the absorption edge is related to the combination between impurities or defects in the Hg₁₋ₓCdₓTe and hydrogen atoms.

IV. Summary and Conclusions

The results of the FTIR measurements on as-grown and hydrogenated Hg₁₋ₓCdₓTe grown on undoped p-CdTe (211) B by MBE showed that the absorption edges shifted to the short wavelength range, and the intensity of the transmittance increased after hydrogenation. The shift of the absorption edge is attributed to be the combination between impurities or defects in the Hg₁₋ₓCdₓTe and hydrogen atoms, and the increase of the transmittance intensity is due to the Hg vacancies being passivated by hydrogen atoms. The results of the Hall effect measuremnts indicated that the variations of the carrier concentration, the mobility, and the resistivity are caused by the decrease of the Hg vacancy defects resulting from the occupation of the Hg vacancies by hydrogen atoms. These results indicate that the crystallinity of the Hg₁₋ₓCdₓTe is improved by hydrogenation and that the type of the p-type Hg₁₋ₓCdₓTe can be changed by hydrogenation.

References
a) Author to whom all correspondence should be addressed.

1. S. J. Pearton, J. W. Corbett, and T. S. Shi, Appl. Phys. A **43**, 153 (1987).
2. R. Mostefaoui, J. Chevallier, A. Jalil, J. C. Pesant, C. W. Tu, and R. F. Kopf, J. Appl. Phys. **64**, 207 (1988).